

## PREPARATION OF NANOPOROUS ADSORBENTS FROM BROWN COAL USING ALKALI ACTIVATION AND THERMAL SHOCK

Yu.V. Tamarkina<sup>1\*</sup>, V.A. Kucherenko<sup>1</sup>, T.G. Shendrik<sup>1</sup>, R.D. Mysyk<sup>1</sup>, N.N. Tsyba<sup>2</sup>

<sup>1</sup> *Litvinenko Institute of Physical-Organic and Coal Chemistry  
of National Academy of Sciences of Ukraine  
70 R. Luxemburg Str., Donetsk, 83114, Ukraine*

<sup>2</sup> *Institute of Sorption and Problems of Endoecology of National Academy of Sciences of Ukraine  
13 General Naumov Str., Kyiv, 03164, Ukraine*

*Thermal-shock KOH activation has been used to produce nanoporous activated carbon from brown coal. The specific surface area, total pore volume, volumes of micropores and subnanometer pores were determined for activated carbons prepared at a varied alkali/coal ratio. Thermal shock was demonstrated to be more efficient for the development of surface area with  $S_{BET}$  equaling up to 1700 m<sup>2</sup>/g in comparison to 1000 m<sup>2</sup>/g for thermally-programmed heating. Increasing the KOH/coal ratio in the activated mixture increases the total pore volume, the micropore volume, and also the volume of subnanometer pores. Thermal shock produces nanoporosity at lower KOH/coal ratios than respective low-rate heating processes of KOH activation.*

### INTRODUCTION

Alkali activation is well known as a method for the preparation of activated carbons (ACs) featuring advantages such as high specific surface area, high volume of micropores and subnanopores and narrow pore size distribution [1, 2]. It can be used for processing many precursors such as coal, biomass, nanotubes, coke and pitch. Besides chemical and physical activation, there are also less common methods for developing porosity in carbon materials. One example is the saturation of coconut shell with nitrogen (1.0 MPa) followed by heating to 523–573 K and adiabatic expansion. Such carbon materials have a low surface area (354–663 m<sup>2</sup>/g) but a narrow pore size distribution with the pores preferentially in the subnanometer range (less than 1 nm) [3]. Another example is chemical pretreatment through intercalation-like reactions of anthracite with nitric or perchloric acid followed by heating and physical activation [4, 5]. Pretreatment favors a 2–3 time rise in the pore volume and micropore volume compared to sole physical activation [5]. A third approach is the intercalation of coal followed by thermal shock at 973 K which allows increasing the surface area (from 14 to 521 m<sup>2</sup>/g) and

micropore volume (from 0.01 to 0.17 cm<sup>3</sup>/g) [6, 7] without activation.

All these methods follow a common line: insertion of guest particles into the inner molecular cavities of the precursor framework and pulse removal of those inserted species which “explodes” the framework on the inside and forms micropores. In addition, thermal shock is known to be an efficient procedure for removing inserted species and is widely used for conversion of graphite intercalation compounds into exfoliated graphite [8].

It appears reasonable to suggest that a combination of alkali activation and thermal shock should lead to the formation of micro- and subnanometer pores due to interaction between the organic framework and KOH which is followed by pulse-induced removal of low-molecular species from the lattice. Such species are framework-trapped water molecules and gaseous products formed in the thermal destruction of framework-forming chains.

Brown coal is attractive precursor used for ACs prepared by KOH activation [9–12]. This kind of coal has a high reactivity toward alkalis owing to reactions of carboxylic, phenolic and ester-type groups with KOH to form carboxylates and phenolates. There are examples of high-efficiency AC preparation from Victorian

\* corresponding author [y\\_tamarkina@rambler.ru](mailto:y_tamarkina@rambler.ru)  
ХФТП 2012. Т. 3. № 2

brown coal (Australia) [11] or brown coal of another deposit [12] with the resulting ACs having a sufficiently high specific surface area ( $S_{\text{BET}} \geq 1000 \text{ m}^2 \cdot \text{g}^{-1}$ ) at a moderate alkali/coal ratio (about 1 g/g). Motivated by the high efficiency of brown coal conversion into ACs by KOH activation [9–12], we previously carried out the conversion of Aleksandriya brown coal (Ukraine) under the experimental conditions common to KOH activation [13–15]: the impregnation of brown coal with potassium hydroxide with the following non-isothermal heating up to 1073 K. Finally, the samples were held at 1073 K for 1 h.

This technique allows one to prepare developed-porosity ACs with a BET specific surface area of 800–1000  $\text{m}^2/\text{g}$ , a total pore volume of 0.5–0.6  $\text{cm}^3/\text{g}$ , and a micropore volume of 0.3–0.4  $\text{cm}^3/\text{g}$  at a KOH/coal ratio of 0.5–1.5 g/g [15]. The resulting ACs exhibit a high adsorption capacity toward a methylene blue dye (100–250 mg/g), phenol (50–200 mg/g at an equilibrium concentration of 0.1–1.0 mg/ml), and iodine (1000–1200 mg/g) [14, 16]. The ACs thus made also have a high hydrogen adsorption capacity (3.2 wt. % at 77 K and 0.33 MPa [17]) which is close in value to that measured under the same conditions for other coal-based ACs [18]. In addition, brown coal-derived carbons reveal a high adsorption capacity toward xenon (0.95 g/g at 293 K and 0.35 MPa) [19], iodine and methyl iodide vapor [20] which is an important point in assessing the material as an adsorbent of radioactive isotopes formed in nuclear reactors. All of the above shows commercialization potential of brown coal-derived nanoporous carbons for waste-water purification, hydrogen storage and the protection of nuclear plants against the spontaneous emission of radioactive gases. This stimulates our further interest in tuning the porosity of the resulting materials by changes in the experimental procedure.

In studying the effect of heating on the properties of ACs from brown coal, we unveiled that both the yield in ACs and the specific surface area were increased at lower KOH/coal ratios if thermal shock conditions were applied instead of rather traditionally accepted heating at a low ramp rate (e.g., 4 K/min) [21, 22]. We identify the thermal shock procedure as introducing a brown coal sample in the 1073 K-preheated reactor zone. However, the literature

data do not reveal such a procedure to be conducted for porosity formation in the KOH-activation of brown coal. We demonstrate that thermal shock allows us preparing somewhat different material and give a detailed account of nanoporosity development under such a procedure.

## EXPERIMENTAL

### *Parent and KOH impregnated coal.*

Aleksandriya brown coal (Kyrovograd region, Ukraine) was used as parent coal whose characteristics are as follows (%):  $W^a$  12.4;  $A^d$  11.7;  $V^{\text{daf}}$  57.6;  $C^{\text{daf}}$  70.4;  $H^{\text{daf}}$  6.0;  $S^{\text{daf}}$  3.8;  $N^{\text{daf}}$  2.0;  $O^{\text{daf}}$  17.8. All the experiments below were performed using a fraction of 0.5–1.0 mm.

The coals were impregnated as follows: a preliminarily dried coal sample (378 K, 2 h) was mixed with a 30 wt % aqueous solution of potassium hydroxide ( $d = 1.29 \text{ g}/\text{cm}^3$ ) and held for 24 h at room temperature. An amount of aqueous KOH solution was chosen such as to meet the required KOH/coal mass ratio (denoted further as  $R_{\text{KOH}}$ ). The sample was then dried at 393 K until constant weight. In reference experiments, a coal sample was soaked with water taken in an amount corresponding to that of alkali solution then held for 24 h and finally dried following the same procedure as for the KOH solutions.

**Preparation of AC.** ACs were prepared by heating the parent or KOH-impregnated coal samples in a vertical tubular steel reactor (a chamber volume of 0.2  $\text{dm}^3$ ). The following stepwise activation procedure was adopted with all the steps being conducted under an argon flow of 2  $\text{dm}^3/\text{h}$ : a sample of 10 g was introduced into the reactor zone preheated up to 1073 K (thermal shock), then held at 1073 K for 1 h, and finally cooled down to room temperature. For comparison, a series of AC samples were made using a low heating rate of 4 K/min at the stage 1 of the technique (instead of thermal shock), steps 2 and 3 remaining unchanged. After activation, the samples were washed off first with distilled water, then with a 0.1 M HCl solution, and once again with water until the negative response of  $\text{Cl}^-$  ions against  $\text{AgNO}_3$ . The samples were finally dried at  $378 \pm 278 \text{ K}$ . Activated carbons made from parent coal are referred to as AC if no KOH was used and AC-K( $R_{\text{KOH}}$ ) if KOH was used for activation. For instance, AC-K(1.0)

abbreviates an AC made at a KOH/coal ratio  $R_{\text{KOH}} = 1.0 \text{ g/g}$ .

**Characterization of pore structure.** The pore structure was explored by the analysis of  $\text{N}_2$  adsorption/desorption isotherms for the samples outgassed at 473 K for 20 h. The isotherms were recorded at 77 K using a Quantachrome Autosorb 6B instrument. The specific surface area  $S_{\text{BET}}$  ( $\text{m}^2/\text{g}$ ) was determined from the BET analysis of the isotherm portion corresponding to a relative  $\text{N}_2$  pressure  $p/p_0$  below 0.3 [23]. The total pore volume  $V_{\Sigma}$  ( $\text{cm}^3/\text{g}$ ) was determined using the amount of nitrogen adsorbed at  $p/p_0 \sim 1$ .

Mesopore size distribution and the volume of mesopores,  $V_{\text{me}}$  ( $\text{cm}^3/\text{g}$ ), were analyzed by the BJH method [24] using the desorption branch of the  $\text{N}_2$  gas isotherms. The mesopore volume  $V_{\text{me}}$  was determined from the cumulative volume curves by accounting only for the volume of pores in the range of 2–50 nm in diameter.

The micropore volume  $V_{\text{mi}}$  ( $\text{cm}^3/\text{g}$ ) was determined using the Dubinin-Radushkevich method [25]. Micropore size distribution was evaluated by the DFT method [26]. The specific surface area ( $S_{\text{DFT}}$ ) and the volume of subnanometer pores less than 1 nm ( $V_{1\text{nm}}$ ) were determined from the DFT cumulative curve for the specific surface area and the specific volume respectively.

## RESULTS AND DISCUSSION

**Yield of activated carbons.** The yield of ACs is decreased almost linearly with increasing the KOH/coal ratio (Fig. 1). At  $R_{\text{KOH}} > 0.5 \text{ g/g}$ , the yield of ACs has higher values under the thermal shock conditions as compared to the respective data for low-rate heating. When low-rate heating is applied, the increase in AC yield at low  $R_{\text{KOH}}$  values can be supposed to arise due to the predominance of condensation-related processes enhanced by potassium cations or potassium metal formed on reducing  $\text{K}^+$  ions by the electrons of the carbon framework [27, 28]. Such condensation reactions were established on heating various coals with sodium hydroxide [29] or polyarenes with potassium hydroxide (e.g., the condensation of benzanthrone into violanthrone at the temperature above 473 K [30]). The condensation reactions are known to induce the formation of additional cross-links in the carbon framework.

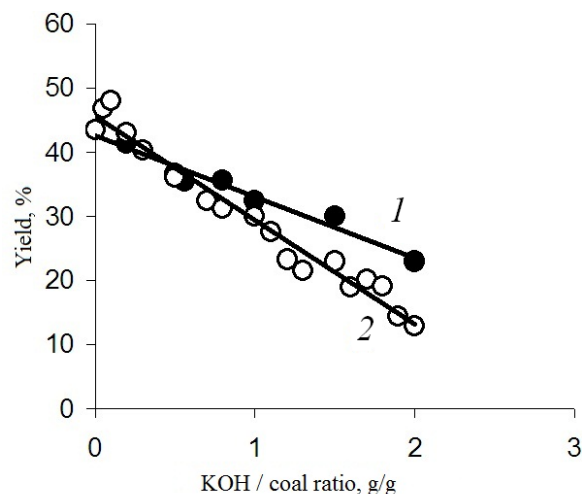


Fig. 1. Yields of activated carbons prepared by thermal shock (1) and low-rate heating (2)

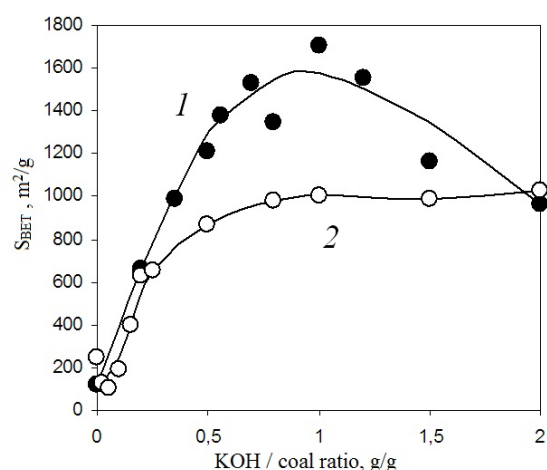


Fig. 2. Specific surface area of activated carbons produced under thermal shock (1) and low-rate heating (2)

**Specific surface area.** One can see easily from Fig. 2 that thermal shock induces higher  $S_{\text{BET}}$  values in a  $R_{\text{KOH}}$  range of 0.5–1.5 g/g only. The samples prepared at  $R_{\text{KOH}} < 0.2 \text{ g/g}$  have low  $S_{\text{BET}}$  values whereas at relatively high KOH/coal ratios ( $R_{\text{KOH}} = 2.0 \text{ g/g}$ ) there is almost no difference in  $S_{\text{BET}}$  of the samples prepared under either the thermal shock or low-rate heating conditions.

Therefore, we conclude from the data of Fig. 2 that it does not make great sense to prepare ACs at the KOH/coal ratios above 1 g/g. For low-rate heating, there is a drop in  $S_{\text{BET}}$  values at  $R_{\text{KOH}}$  between 0 and 0.2 g/g. Note that this drop in  $S_{\text{BET}}$  values corresponds to the rise in AC yield and both features are caused by the polycondensation reactions resulting in a rigid cross-linked framework. Taking into account the

decrease in  $S_{\text{BET}}$  values at a low alkali/coal ratio (Fig. 2), we decided not to proceed with the thermal-shock preparation of ACs at  $R_{\text{KOH}} < 0.2$  g/g since the condensation reactions can reasonably be expected to occur also under thermal shock, not favouring developed porosity.

**Adsorption isotherms.** As can be seen from Fig. 3, at low  $p/p_0$  there is a drastic increase in the amount of adsorbed nitrogen, *i.e.* the initial portion of the adsorption isotherms can be related to type I isotherms [31]. The shape of isotherms is in itself indicative of ACs being essentially microporous.

All the isotherms are characterized by the presence of H4-type hysteresis loops according to the IUPAC guidelines [31]. According to this type of hysteresis, the adsorption and desorption branches in Fig. 3 are nearly parallel to the horizontal axis over a wide range of  $p/p_0$ . Such a type of hysteresis loops is associated with the presence of narrow slit-like pores but is also

indicative of substantial microporosity in the case of type I isotherms.

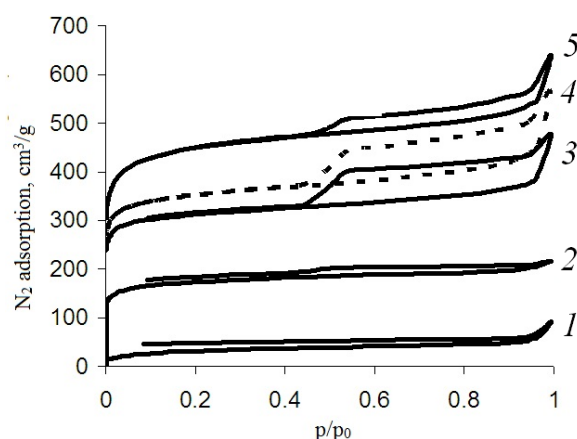


**Fig. 3.** Nitrogen adsorption-desorption isotherms at 77 K for activated carbons derived from brown coal under thermal shock: 1 – AC; 2 – AC-K(0.2); 3 – AC-K(0.5); 4 – AC-K(0.8); 5 – AC-K(1.0)

**Table.** Porosity characterization of nanoporous materials AC and AC-K

Parameter	Material				
	AC	AC-K(0.2)	AC-K(0.5)	AC-K(0.8)	AC-K(1.0)
$S_{\text{BET}}$ , m <sup>2</sup> /g	123	664	1212	1348	1706
$S_{\text{DFT}}$ , m <sup>2</sup> /g	74	515	1356	1411	1680
$V_{\Sigma}$ , cm <sup>3</sup> /g	0.14	0.34	0.74	0.88	1.00
$V_{\text{mi}}$ , cm <sup>3</sup> /g	0.03	0.25	0.41	0.48	0.71
$V_{\text{mi}}/V_{\Sigma}$	0.22	0.74	0.55	0.55	0.72
$V_{\text{mc}}$ , cm <sup>3</sup> /g	0.035	0.064	0.30	0.35	0.28
$V_{\text{mc}}/V_{\Sigma}$	0.25	0.19	0.40	0.40	0.28
$V_{1\text{nm}}$ , cm <sup>3</sup> /g	0.01	0.13	0.35	0.36	0.40
$V_{1\text{nm}}/V_{\Sigma}$	0.05	0.38	0.48	0.40	0.41

Furthermore, for AC and AC-K(0.2), we observe low pressure hysteresis, extending to the lowest attainable values of  $p/p_0$  (see curves 1, 2 in Fig. 3). Such behavior can be caused by the swelling of carbon framework, the irreversible uptake of nitrogen molecules in pores or even chemical interaction of the adsorbate with carbon surface [31]. For our brown coal-derived carbons, we believe that topochemical reactions are unlikely and also the swelling can be neglected due to the rigidity of the framework. Thus, the presence of low-temperature hysteresis is most likely associated with the irreversible trapping of nitrogen molecules in the smallest

micropores, possibly those with pore entrances less than 0.4 nm.

Increasing the KOH/coal ratio gives rise to low pressure hysteresis becoming less apparent, with its complete disappearance for samples AC-K(0.8) and AC-K(1.0).

**Pore structure characterization.** The most important porosity features are summarized in Table. If activated carbon is produced by heating brown coal at 1073 K without alkali, it is characterized by a poorly developed porosity (material AC).  $S_{\text{BET}}$  is only 123 m<sup>2</sup>/g, the total pore volume and the volume of micropores are also not too large but the micropores amount to

22 % of the total porosity. The micropores are mostly 1–2 nm wide pores with only 1 % of the pores corresponding to pores less than 1 nm.

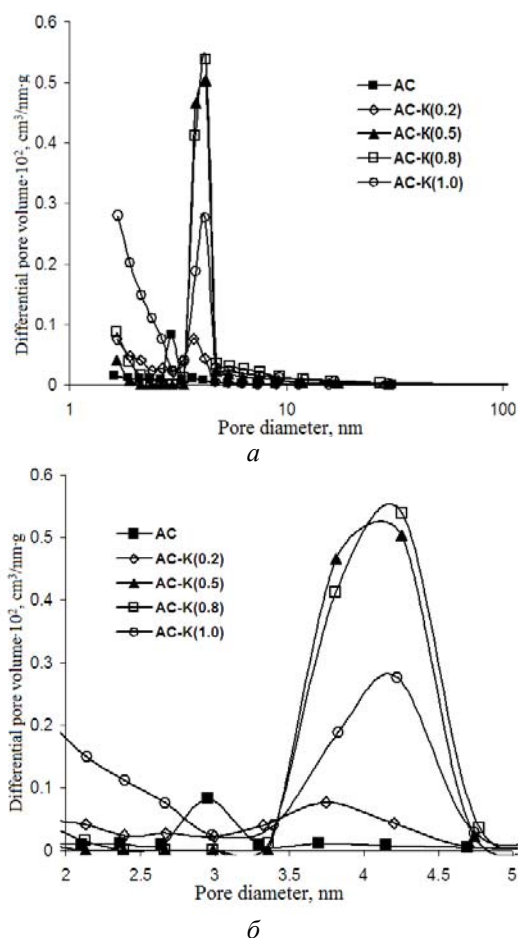


**Fig. 4.** BJH mesopore size distribution (a); close-up of the BJH pore size distribution for pore size between 2 and 5 nm (b)

The AC-K materials prepared by KOH activation feature more developed porosity and a more substantial pore volume. Thus, the specific area of the AC materials rises from 123 to 1706 m<sup>2</sup>/g on increasing the KOH/coal ratio in the impregnated coal which represents a 14-time increase in  $S_{\text{BET}}$  values (Fig. 2, line 1). Note also that  $S_{\text{BET}}$  and  $S_{\text{DFT}}$  have close values.

Increasing the KOH/coal ratio from 0 to 1 g/g results in a 7-time rise in the total pore volume (0.14 to 1.00 cm<sup>3</sup>/g). At the same time, the micropore volume increases by a factor of 24 (0.03 to 0.71 cm<sup>3</sup>/g). All the AC-K samples have no or a very small amount of macropores (not more than 0.07 $V_{\Sigma}$ ). As to mesopores, their quantity rises progressively with  $R_{\text{KOH}}$  but there is no evident trend in their contribution to the total pore volume.

We also evaluated the volume ( $V_{1\text{nm}}$ ) of pores less than 1 nm and their fraction (defined as  $V_{1\text{nm}}/V_{\Sigma}$ ) as a function of the alkali/coal ratio. We draw particular attention to subnanometer pores since they are of utmost importance to both high hydrogen adsorption capacity [32] and high electrochemical capacitance [33]. In other words, the larger the volume of subnanometer pores, the better the nanoporous carbon.

The volume of subnanometer pores increases by a factor of 40, their fraction ( $V_{1\text{nm}}/V_{\Sigma}$ ) in the total pore volume rises sharply in the  $R_{\text{KOH}}$  range of 0 to 0.5 g/g whereas the  $V_{1\text{nm}}/V_{\Sigma}$  values decrease slightly at  $R_{\text{KOH}} \geq 0.5$  g/g. Hence, the alkali activation of brown coal under thermal shock is capable to produce materials with developed subnanometer porosity. We believe that our experimental procedure can further be tuned as to maximizing the volume of subnanometer pores.

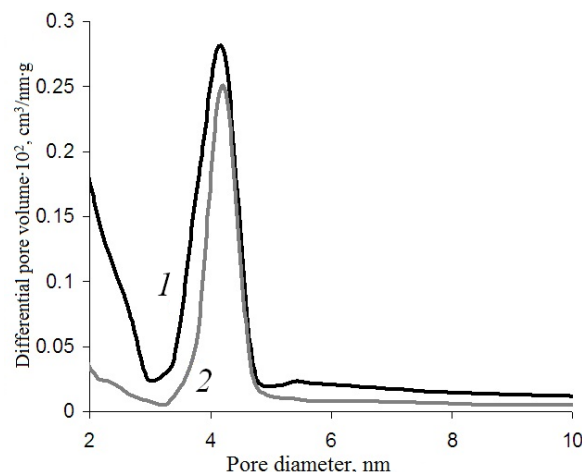


**Fig. 5.** The BJH mesopore size distribution of the carbons prepared under thermal shock (1) and low-rate heating (2).  $R_{\text{KOH}} = 1$  g/g for both cases

**Mesopore size distribution.** Fig. 4 demonstrates that the pore size distribution of material AC has a maximum for 3 nm - wide mesopores whereas the distribution in the other pore size regions is quite uniform. The pore size distribution of AC-K(0.2) carbon has a peak at 3.7 nm. The peak is shifted to about 4.2–4.3 nm for material AC-K(0.5) and does not change position further for materials AC-K(0.8) and AC-K(1.0).

Fig. 5 compares activated carbons prepared at the same KOH/coal ratio ( $R_{\text{KOH}} = 1$  g/g) but under different heating conditions. The mesopore size distributions of both carbons are rather similar exhibiting maxima at the same pore

diameter of 4.2 nm. The main differences between the carbons are apparent for pore size less than 3 nm with more small pores for the carbon prepared under thermal-shock KOH activation.

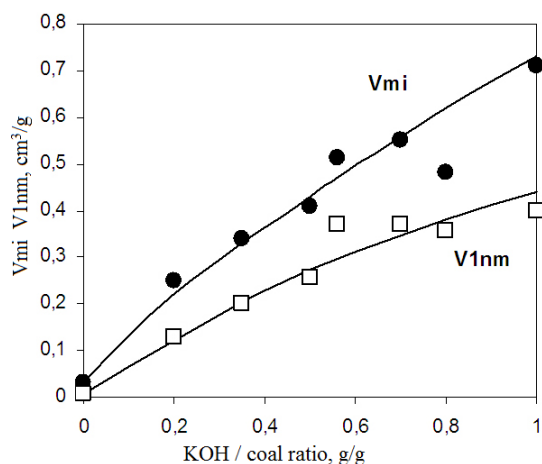


**Fig. 6.** The volume of micropores and subnanopores vs the KOH/coal ratio

**Micropore size distribution.** Figs. 6 and 7 show that the micropore structure is greatly dependent on the KOH/coal ratio. The micropore volume  $V_{mi}$  increases up to  $0.71 \text{ cm}^3/\text{g}$  (corresponding to 71 % of the total pore volume) as  $R_{\text{KOH}}$  rises (Fig. 6). A similar trend can be followed for subnanometer pores; they make up 40–50 % of all the porosity for ACs prepared at  $R_{\text{KOH}} = 0.5\text{--}1.0 \text{ g/g}$  (Table).

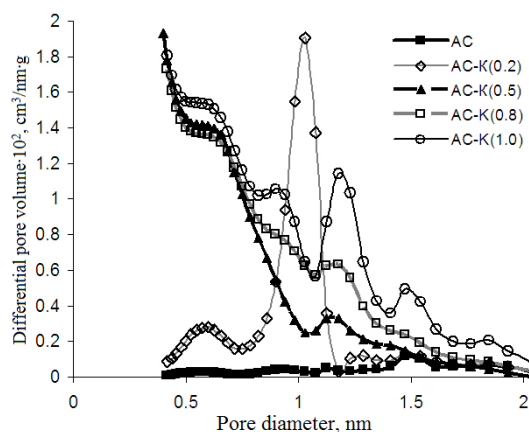


**Fig. 7.** DFT micropore size distribution for materials AC and AC-K

The sample AC is characterized by a relatively uniform micropore distribution, with a little peak for pores of 1.5 nm (Fig. 7). For the sample AC-K(0.2), most pores have a diameter of 1 nm whereas there are much less pores with a diameter  $< 0.7 \text{ nm}$  and  $> 1.5 \text{ nm}$ . Increasing the KOH/coal ratio from 0.2 to

0.5 g/g induces drastic changes in micropore size distribution: the maximum at 1 nm disappears with mostly developing pores being those less than 0.7 nm in diameter. Increasing the KOH/coal ratio from 0.5 to 1.0 g/g does not considerably increase the amount of pores less than 0.7 nm but does strongly enhance the formation of pores which are 0.9, 1.2, 1.5 and 1.8 nm in diameter (Fig. 7). This can arise owing to somewhat stronger interactions of alkali with the carbon framework under thermal shock which can lead to a certain enlargement of the smallest pores.

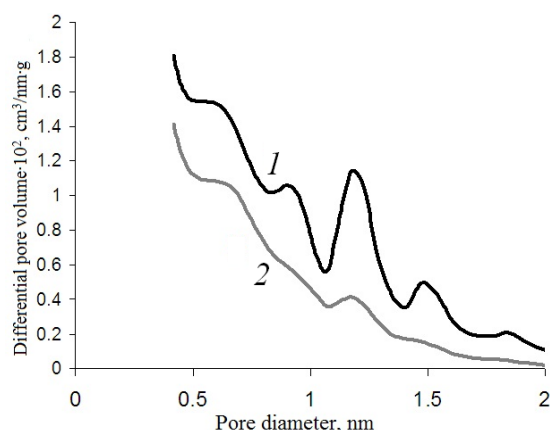


**Fig. 8.** Comparison of DFT micropore size distributions for carbons prepared using thermal shock (1) and low-rate heating (2)

Fig. 8 compares the micropore size distributions of carbons prepared using thermal shock and low-rate heating at the same KOH/coal ratio ( $R_{\text{KOH}} = 1 \text{ g/g}$ ). Switching to the thermal shock conditions gives rise to an increased volume of micropores and somewhat different pore size distribution with pores over 1 nm being developed to a much greater extent for thermal-shock activated carbon. The distribution of micropores less than 1 nm is similar for both carbons.

We further propose a mechanism for developing porosity in brown coal-derived carbons under thermal shock through thermally-initiated reactions involving KOH. We build upon the common concepts of alkali activation [1, 2, 27–29, 34] and thermal-shock exfoliation of graphite intercalation compounds [4, 6–8, 35]. Thus, we propose the first event to be a high-temperature pulse formation of low-molecular products from thermally labile structural fragments such as phenolate and carboxylate functionalities formed in the alkali impregnation of brown coal. This is followed by a pulse evolution of molecules ( $\text{H}_2\text{O}$ ,  $\text{CO}$ ,  $\text{CO}_2$ ,  $\text{CH}_4$ ,

C<sub>2</sub>H<sub>6</sub>, and other gases) from the framework producing internal cavities of molecular size.

Those cavities do not collapse since they are kept up by the species present in the precursor framework such as K<sup>+</sup>, OH<sup>-</sup>, KOH, and also by K<sub>2</sub>O and K<sub>2</sub>CO<sub>3</sub> formed through thermally initiated reactions with KOH [2, 27, 28, 36]. Simultaneously, there is a build-up of internal C-C cross-links which stabilizes the formed microporosity and provides the porous framework with rigidity.

### CONCLUSIONS

We have found that the KOH activation of Aleksandriya brown coal under thermal shock (1073 K) is capable to produce nanoporous carbons with a high surface area (up to 1700 cm<sup>2</sup>/g), a total pore volume of about 1 cm<sup>3</sup>/g and a micropore volume of 0.7 cm<sup>3</sup>/g. This process is more efficient than slower thermally-programmed heating up to 1073 K adopted in most conventional methods for alkali activation.

Increasing the KOH/coal ratio in the activated mixture increases the micropore volume (0.03 to 0.71 cm<sup>3</sup>/g) and the volume of subnanometer pores (0.01 to 0.40 cm<sup>3</sup>/g). The thermal-shock KOH activation produces activated carbons with more developed porosity but pore size distribution does not differ significantly from that for the carbons prepared under low-rate heating conditions. Thermal shock additionally promotes the formation of pores of 0.6, 1.2, 1.5 nm in diameter.

Thermal shock allows developing nanoporosity at lower KOH/coal ratios (0.5–1.0 g/g) than those for the respective low-rate heating processes of KOH activation. This can bring a technological advantage since a lower KOH consumption decreases the amount of alkali solutions formed on washing off activated carbons.

In summary, activated carbons prepared by KOH activation of Aleksandriya brown coal were demonstrated to have a moderately developed nanoporosity with a fraction of subnanometer pores of 0.4–0.5. Therefore, we can expect that our materials hold promise for use in hydrogen storage systems, energy storage in electrochemical capacitors, and waste-water purification.

### REFERENCES

1. Marsh H, Rodriguez-Reinoso F. Activated carbon. – Amsterdam: Elsevier; 2006. – 542 p.
2. Lillo-Rodenas M.-A., Cazorla-Amoros D., Linares-Solano A. Understanding chemical reactions between carbons and NaOH and KOH. An insight into the chemical activation mechanism // Carbon. – 2003. – V. 41, N 2. – P. 267–275.
3. Su W., Zhou L., Zhou Y. Preparation of microporous activated carbon from coconut shells without activated agents // Carbon. – 2003. – V. 41, N 4. – P. 861–863.
4. Lyubchik S.B., Benaddi H., Shapranov V.V., Béguin F. Activated carbons from chemically treated anthracite // Carbon. – 1997. – V. 35, N 1. – P. 162–165.
5. Lyubchik S.B., Galushko L.Ya., Rego A.M. et al. Intercalation as an approach to the activated carbon preparation from Ukrainian anthracites // J. Phys. Chem. Solids. – 2004. – V. 65, N 2–3. – P. 127–132.
6. Albinia A., Furdin G., Béguin F. et al. Exfoliation and textural modification of anthracites // Carbon. – 1996. – V. 11, N 11. – P. 1329–1334.
7. Furdin G. Exfoliation process and elaboration of new carbonaceous materials // Fuel. – 1998. – V. 77, N 6. – P. 479–485.
8. Inagaki M., Tashiro R., Washino Y., Toyoda M. Exfoliation process of graphite via intercalation compounds with sulfuric acid // J. Phys. Chem. Solids. – 2004. – V. 65, N 2–3. – P. 133–137.
9. Durie R.A., Schafer H. N. S. The production of active carbon from brown coal in high yields // Fuel. – 1979. – V. 58, N 6. – P. 472–476.
10. Guy P.J., Verheyen T.V., Heng S. et al. Physical properties of activated carbons derived from alkali treated Victorian brown coals. Proceedings, Int. Conf. on Coal Science (Tokyo, Japan). – 1989. – V. 1. – P. 21–24.
11. Guy P.J., Perry G.J. Victorian brown coal as a source of industrial carbons: a review // Fuel. – 1992. – V. 71, N 10. – P. 1083–1086.
12. Amarasekera G., Scarlett M.J., Mainwaring D.E. Development of microporosity in carbons derived from alkali digested coal // Carbon. – 1998. – V. 36, N 7–8. – P. 1071–1078.
13. Tamarkina Y.V., Bovan L.A., Kucherenko V.A. Properties of the solid thermolysis products of brown coal impregnated with an alkali // Solid fuel chem. – 2008. – V. 42, N 4. – P. 202–207.
14. Tamarkina Y.V., Maslova L.A., Khabarova T.V., Kucherenko V.A. Adsorption properties of carbon materials produced by thermolysis

- of brown coal in the presence of alkali metal hydroxides // *Russ. J. Appl. Chem.* – 2008. – V. 81, N 7. – P. 1167–1170.
15. *Shendrik T.G., Tamarkina Y.V., Khabarova T.V. et al.* Formation of the pore structure of brown coal upon thermolysis with potassium hydroxide // *Solid Fuel Chem.* – 2009. – V. 43, N 5. – P. 309–313.
  16. *Isaeva L.N., Tamarkina Y.V., Bovan D.V., Kucherenko V.A.* Phenol adsorption on active carbons prepared under thermolysis of brown coal with potassium hydroxide // *J. Siberian Fed. Univ. Chemistry.* – 2009. – V. 2. – P. 25–32.
  17. *Tamarkina Y.V., Kolobrodov V.G., Shendrik T.G. et al.* Properties of adsorbents prepared by the alkali activation of Aleksandriisk brown coal // *Solid Fuel Chem.* – 2009. – V. 43, N 4. – P. 233–237.
  18. *Jorda-Beneyto M., Suarez-Garcia F., Lozano-Castello D. et al.* Hydrogen storage on chemically activated carbons and carbon nanomaterials // *Carbon.* – 2007. – V. 45, N 2. – P. 293–303.
  19. *Shendrik T.G., Kolobrodov V.G., Tamarkina Y.V., Kucherenko V.A.* Hydrogen and xenon adsorption on nanoporous materials from brown coal // XI Int. Conference “Hydrogen materials science and chemistry of carbon nanomaterials (Yalta, Ukraine, 2009): Extended Abstr. – P. 636–637.
  20. *Tamarkina Yu.V., Shendrik T.G.* Adsorbents from brown coal for ecotoxicants trapping from air and waste water // *Ecology and Industry.* – 2010. – N 4. – P. 40–43. (in Russian).
  21. *Pat. 61059 Ukraine, C 01 B 31/08.* Carbon porous material from brown coal and method for producing it / Tamarkina Yu.V., Khabarova T.V., Shendrik T.G., Kucherenko V.A. – Appl. No u201014280, Filled 29.11.2010, Publ. 11.07.2011. – 4 p. (in Ukrainian).
  22. *Kucherenko V.A., Shendrik T.G., Tamarkina Yu.V., Mysyk R.D.* Nanoporosity development in the thermal shock KOH activation of brown coal // *Carbon.* – 2010. – V. 48. – P. 4556–4558.
  23. *Brunauer S., Emmett P.H., Teller E.* Adsorption of gases in multimolecular layers // *J. Am. Chem. Soc.* – 1938. – V. 60, N 2. – P. 309–319.
  24. *Barret E.P., Joyner L.C., Halenda P.P.* The determination of pore volume and area distributions in porous substances. I. Computations from nitrogen isotherms // *J. Am. Chem. Soc.* – 1951. – V. 73, N 1. – P. 373–380.
  25. *Dubinin M.M.* Fundamentals of the theory of adsorption in micropores of carbon adsorbents: characteristics of their adsorption properties and microporous structures // *Carbon.* – 1989. – V. 27, N 3. – P. 457–467.
  26. *Lastoskie C., Gubbins K.E., Quirke N.* Pore size distribution analysis of microporous carbons: a density functional theory approach // *J. Phys. Chem.* – 1993. – V. 97, N 18. – P. 4786–4796.
  27. *Diaz-Teran J., Nevskaja D.M., Fierro J.L.G. et al.* Study of chemical activation process of a lignocellulosic material with KOH by XPS and XRD // *Microp. Mesop. Mater.* – 2003. – V. 60, N 1–3. – P. 173–181.
  28. *Raymundo-Pinero E., Azais P., Cacciaguerra T. et al.* KOH and NaOH activation mechanisms of multiwalled carbon nanotubes with different structural organization // *Carbon.* – 2005. – V. 43, N 4. – P. 786–795.
  29. *Yamashita Y., Ouchi K.* Influence of alkali on the carbonization process. II. Carbonization of various coals and asphalt with NaOH // *Carbon.* – 1982. – V. 20, N 1. – P. 47–53.
  30. *Clar E.* Polycyclic Hydrocarbons. London: Academic Press, 1964. – 391 p.
  31. *Sing K.S.W., Everett D.H., Haul R.A.W. et al.* Reporting physisorption data for gas/solid systems with special reference to the determination of surface area and porosity // *Pure Appl. Chem.* – 1985. – V. 57, N 4. – P. 603–619.
  32. *Xia K., Gao Q., Wu C. et al.* Activation, characterization and hydrogen storage properties of the nanoporous carbon CMK-3 // *Carbon.* – 2007. – V. 45, N 10. – P. 1989–1996.
  33. *Chmiola J., Yushin G., Gogotsi Y. et al.* Anomalous increase in carbon capacitance at pore sizes less than 1 nanometer // *Science.* – 2006. – V. 313, N 5794. – P. 1760–1763.
  34. *Yoshizawa N., Maruyama K., Yamada Y. et al.* XRD-evaluation of KOH activation process and influence of coal rank // *Fuel.* – 2002. – V. 81, N 15. – P. 1717–1722.
  35. *Xue R., Shen Z.* Formation of graphite-potassium intercalation compounds during activation of MCMB with KOH // *Carbon.* – 2003. – V. 41, N 9. – P. 1862–1864.

36. Qiao W., Yoon S.H., Mochida I. KOH activation of needle coke to develop activated carbons for high-performance

EDLC // Energy & Fuels. – 2006. – V. 20, N 4. – P. 1680–684.

Received 26.12.2011, accepted 26.03.2012

### **Одержання нанопоруватих адсорбентів з бурого вугілля лужною активацією із застосуванням теплового удару**

**Ю.В. Тамаркіна, В.О. Кучеренко, Т.Г. Шендрік, Р.Д. Мисик, М.М. Циба**

*Інститут фізико-органічної хімії і вуглехімії ім. Л.М. Литвиненка  
Національної академії наук України  
вул. Р. Люксембург, 70, Донецьк, 83114, Україна, у\_tamarkina@rambler.ru  
Інститут сорбції та проблем ендоекології Національної академії наук України  
вул. Генерала Наумова, 13, Київ, 03164, Україна*

*Методом лужної активації КОН із застосуванням теплового удару одержано нанопоруватий матеріал з бурого вугілля. Для зразків активованого вугілля, сформованих при варіюванні співвідношення луг/вугілля, було визначено площу питомої поверхні, сумарний об'єм пор, об'єми мікро- та субнанопор. Показано, що нагрівання в режимі теплового удару більш ефективно для розвинення поверхні;  $S_{\text{ВЕТ}}$  сягають  $1700 \text{ м}^2/\text{г}$ , тоді як при термопрограмованому нагріванні –  $1000 \text{ м}^2/\text{г}$ . Збільшення співвідношення КОН/вугілля у суміші, що активується, сприяє збільшенню сумарного об'єму пор, об'єму мікропор, а також об'єму субнанопор. Тепловий удар стимулює розвинення нанопоруватості при більш низьких співвідношеннях КОН/вугілля порівняно з повільним нагріванням.*

### **Получение нанопористых адсорбентов из бурого угля щелочной активацией с применением теплового удара**

**Ю.В. Тамаркина, В.А. Кучеренко, Т.Г. Шендрик, Р.Д. Мысык, Н.Н. Циба**

*Інститут фізико-органічної хімії і вуглехімії ім. Л.М. Литвиненко  
Національної академії наук України  
вул. Р. Люксембург, 70, Донецьк, 83114, Україна, у\_tamarkina@rambler.ru  
Інститут сорбції і проблем ендоекології Національної академії наук України  
вул. Генерала Наумова, 13, Київ, 03164, Україна*

*Методом щелочной активации КОН с применением теплового удара получен нанопористый материал из бурого угля. Для образцов активированных углей, сформированных при варьировании соотношения щелочь/уголь, определены площадь удельной поверхности, суммарный объем пор, объемы микро- и субнанопор. Показано, что нагревание в режиме теплового удара более эффективно для развития поверхности;  $S_{\text{ВЕТ}}$  достигают  $1700 \text{ м}^2/\text{г}$ , тогда как при термопрограммируемом нагревании –  $1000 \text{ м}^2/\text{г}$ . Увеличение соотношения КОН/уголь в активированной смеси способствует увеличению суммарного объема пор, объема микропор, а также объема субнанопор. Тепловой удар стимулирует развитие нанопористости при более низких соотношениях КОН/уголь по сравнению с медленным нагревом.*